Calculation of Optimum Angle of Attack to Determine Maximum Lift to Drag Ratio of NACA 63_2-215 Airfoil

Haci Sogukpinar
Department of Energy Systems Engineering,
Faculty of Technology, University of Adiyaman,
Adiyaman 02040, Turkey,
hsogukpinar@adiyaman.edu.tr

Ismail Bozkurt
Department of Mechanical Engineering,
Faculty of Engineering, University of Adiyaman,
Adiyaman 02040, Turkey.
ibozkurt@adiyaman.edu.tr

***Abstract*—Wind energy is an important source to meet future energy needs. Therefore, investigations on wind power technology are progressing rapidly. In this study, numerical simulation of airfoil was conducted to determine optimum angle of attack for horizontal axis wind turbine. This study simulates air flow around inclined NACA 63_2-215 airfoil using SST turbulence model. Lift, drag coefficient, lift to drag ratio and power coefficient around the airfoil were calculated and compared with different velocity. With the increasing of wind velocity, lift and drag coefficient increases and maximum lift to drag ratio starts to increase then degreases again. Maximum lift to drag ratio is reached around 4 degree. Power coefficients were calculated at the speed of 10 m/s and graph was plotted. With the increasing angle of attack pressure difference between upper and lower surface increases.**

***Keywords*— Airfoil characteristics, lift-todrag ratio, high angles of attack**

I. Introduction

Wind energy is the most popular among all the renewable sources of energy. The technology of the wind turbine is progressing rapidly. With increased efficiency and cost improvements, wind energy can clearly play a significant role in the world's future energy. The installation of the wind power plants is increasing rapidly in Europe and around the world. Until 1990 installed wind power capacity only reached 439 MW around Europa. After 1997 installed wind power capacity in Europa started to increase so fast. In 2007 total installed capacity around Europa reached 5700 MW and 128751 MW by 2014 (28 EU Country) [1]. Wind turbine consists of different components. One of the wind turbine components is blade. Recent years, the researchers focus on the improving the aerodynamic performance of wind turbine blade. Rajakumar and Ravindran [2] investigated the lift and drag forces in a wind turbine blade at various sections and the effect of angle of attack on these forces were studied for NACA 4420. Lee et. al. [3] analyzed the effects of idealized local shear flows around a two-dimensional S809 airfoil on its aerodynamic characteristics by using CFD simulations. Various parameters including reference inflow velocity, shear rate, angle of attack, and cord length of the airfoil were examined. Gharali and Johnson [4] simulated an oscillating free stream over a stationary S809 airfoil numerically by using ANSYS Fluent for comparison the laminar-turbulent transition with the realizable k–ε, SST and k–w models. Thumthae and Chitsomboon [5] investigated the numerical simulation of horizontal axis wind turbines with untwisted blade to determine the optimal angle of attack that produces the highest power output. The computational results of the 12^0 pitch was compared favorably with the field experimental data of The National Renewable Laboratory. Lee et. al. [6] evaluated the performance of a blade with blunt airfoil which was adapted at the root. The comparison analysis of results of a baseline and modified blades was performed for different wind speeds. Zanotti et. al. [7] investigated both two and three-dimensional CFD models by using a compressible Navier–Stokes solver for deep dynamic stall experiments carried out on a pitching NACA 23012 airfoil.

Wind turbine blade simulation through Computational Fluid Dynamics (CFD) software offers to aerodynamic blade analysis. In this study, numerical simulation of NACA 63_2-215 airfoil was performed to determine optimum angle of attack. Lift and drag coefficient, lift to drag ratio and power coefficient around airfoil were calculated and compared. With the increasing of wind velocity, lift and drag coefficient increases.

II. MATERIAL AND METHOD

Shear Stress Transport model was introduced in 1994 by F.R. Menter to deal with the strong free-stream sensitivity of the k-omega turbulence model and improve the predictions of adverse pressure gradients. Model is interpreted with in terms of k and w. Calculated two variables, k is the turbulent kinetic energy and w is the rate of dissipation of the eddies. SST model is expressed with the help of equation in terms of k (1) and w (2) [8]

$$\rho\frac{\partial k}{\partial t}+\rho u.\nabla k=P-\rho{\beta_0}^{*}k\omega+\nabla.\left((\mu+\sigma_k\mu_T)\nabla_k\right) \quad (1)$$

$$\rho\frac{\partial \omega}{\partial t}+\rho u.\nabla \omega=\frac{\rho\gamma}{\mu_T}P-\rho\beta\omega^2+\nabla.\left((\mu+\sigma_\omega\mu_T)\nabla_\omega\right)+2(1-f_{v1})\frac{\rho\sigma_{\omega^2}}{\omega}\nabla\omega.\nabla k \quad (2)$$

Turbulence viscosity can be represented as equation (3):

$$\mu_T = \frac{\rho a_1 k}{\max(a_1\omega, S f_{v2})} \qquad (3)$$

Where, S is the overall magnitude of the mean velocity gradients and represented with the help of equation (4)

$$S = \sqrt{2S_{ij}S_{ij}} \qquad (4)$$

The model constants are expressed through interposition of appropriate inner and outer values and the interposition functions f_{v1} and f_{v2} are represented as equation (5) and (6),

$$f_{v1} = \tanh\left(min \left[\frac{max\left(\frac{\sqrt{k}}{\beta_0{}^* \omega l_\omega}, \frac{500\mu}{\rho\omega l_\omega{}^2}\right),\ 4\rho\sigma_{\omega 2}k}{\max(\frac{2\rho\sigma_{\omega 2}}{\omega}\nabla\omega.\nabla k, 10^{-10}) l_\omega{}^2} \right]^4 \right) \qquad (5)$$

$$f_{v2} = tanh\left(max\left(\frac{\sqrt{k}}{\beta_0{}^*\omega l_\omega}, \frac{500\mu}{\rho\omega l_\omega{}^2}\right)^2 \right) \qquad (6)$$

SST default model constants are represented by [8],

$$\beta_1 = 0.075, \gamma_1 = \frac{5}{9}, \sigma_{k1} = 0.85, \sigma_{\omega 1} = 0.5, \beta_2 = 0.0828, \gamma_2 = 0.44, \sigma_{k2} = 1.0, \sigma_{w2} = 0.856, \beta_0{}^* = 0.09, \sigma_1 = 0.31 \qquad (7)$$

The computational conditions are as shown in Table 1.

TABLE I. COMPUTATIONAL CONDITION

Density	$1.2043 kg/m^3$
Wind speed	10, 20, 30, 40, 50 m/s
Angle of attack (Deg)	-6,-5,-4,-3,-2,-1, 0,1,2,3,4,5,6,7,8,9,10
Turbulent kinetic energy	$4.1840E-7 m^2/s^2$
Specific dissipation rate	2.7778 1/s
Chord lengths	1.8 m
Temperature	193 K
Reference pressure	1 atm
Reference Length	0.2 m

In this study incompressible flow is reputed, and flow is assumed to be turbulent over entire airfoil. Computational domain is located 100 chord length away from leading edge and 200 chord length away from trailing edge. Boundary condition and flow domain are shown in Figure 1.

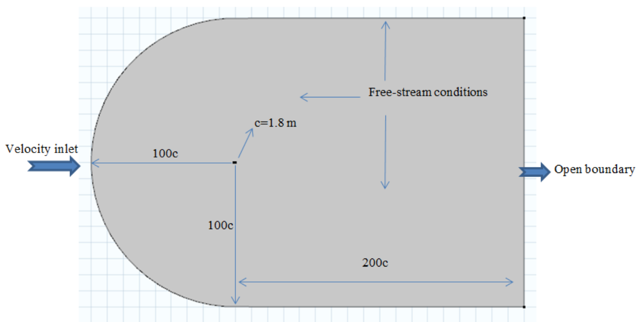

Figure 1. Boundary condition and flow domain

A no-slip condition is applied on the airfoil surface. Computational grid is shown in Figure 2.

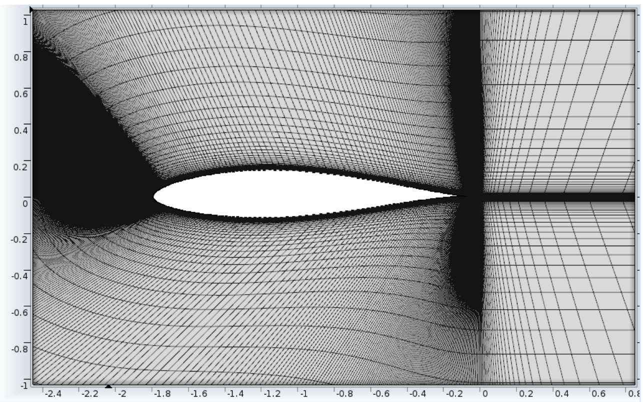

Figure 2. Domain of computational grid

Computational domain was divided into four different regions and high size-ratio mesh was applied between endmost and wall element.

III. RESULTS AND DISCUSSION

This study was conducted using COMSOL 4.3b simulation software for NACA 63_2-215 airfoil. Numerical calculations were carried out at different velocity and range of velocity is listed at Table 1. The objective of this calculation is to find optimum angle of attack to obtain maximum lift to drag ratio. Also in this study, pressure coefficient formed around of NACA 63_2-215 airfoil were calculated and compared with different angle of attack of airfoil. Angle of attack for inclined airfoil is given in Table 1. Lift coefficient for different velocities were calculated and shown in Figure 3.

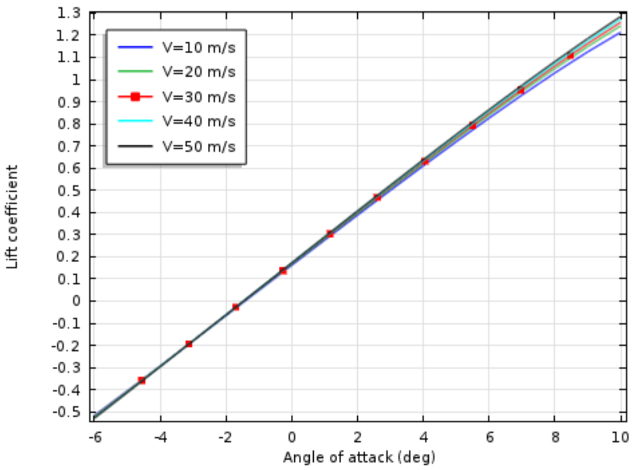

Figure 3. Lift coefficient versus angle of attacks

According to Figure 3, with increasing of velocity, lift coefficient increases. But as the speed of air exceeds 30 m/s, lift coefficient increment decreases. At low angle, lift coefficient for each case so similar but at high angle lift coefficient difference can be seen clearly. Figure 4 shows drag coefficient with respect to angle of attack and with increasing of relative velocity drag coefficient decreases. With the increasing of relative velocity, drag increment degreases also.

Maximum drag coefficient observes at the speed of 10 m/s and minimum at 50 m/s. Minimum drag coefficient observes at around -1 to 0 degree and maximum at 10 degree. As the angle of attack exceeds 6°, drag coefficient increases rapidly.

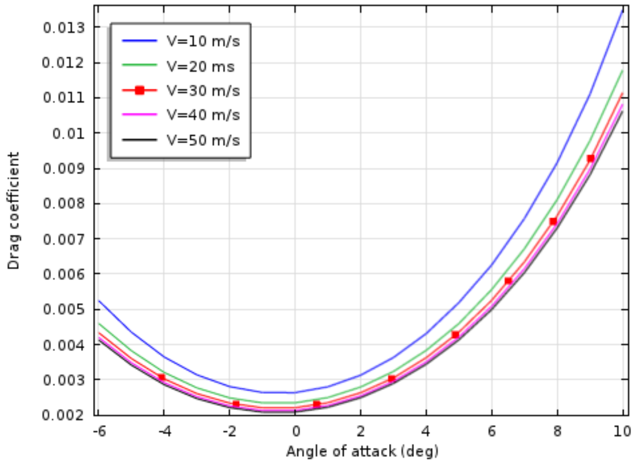

Figure 4. Drag coefficient versus angle of attack

Lift to drag ratio with the angle of attack is shown in Figure 5. With the increasing of angle of attack, lift to drag ratio increase first and then decreases. Maximum lift to drag ratio is reached at around 4° for all speed. With the increasing of wind speed, maximum lift to drag ratio increases also. Maximum lift to drag ratio is observed at the speed of 50 m/s and minimum at 10 m/s. In this study lift to drag ratio increases in proportion to wind speed. Pressure coefficients of airfoil are shown in Figure 6a-r.

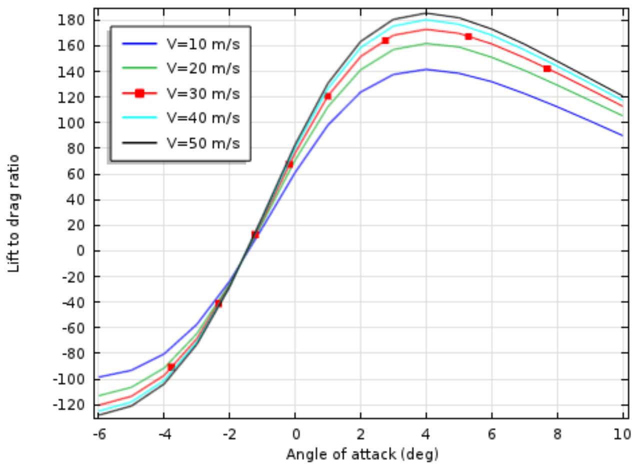

Figure 5. lift to drag ratio versus angle of attack

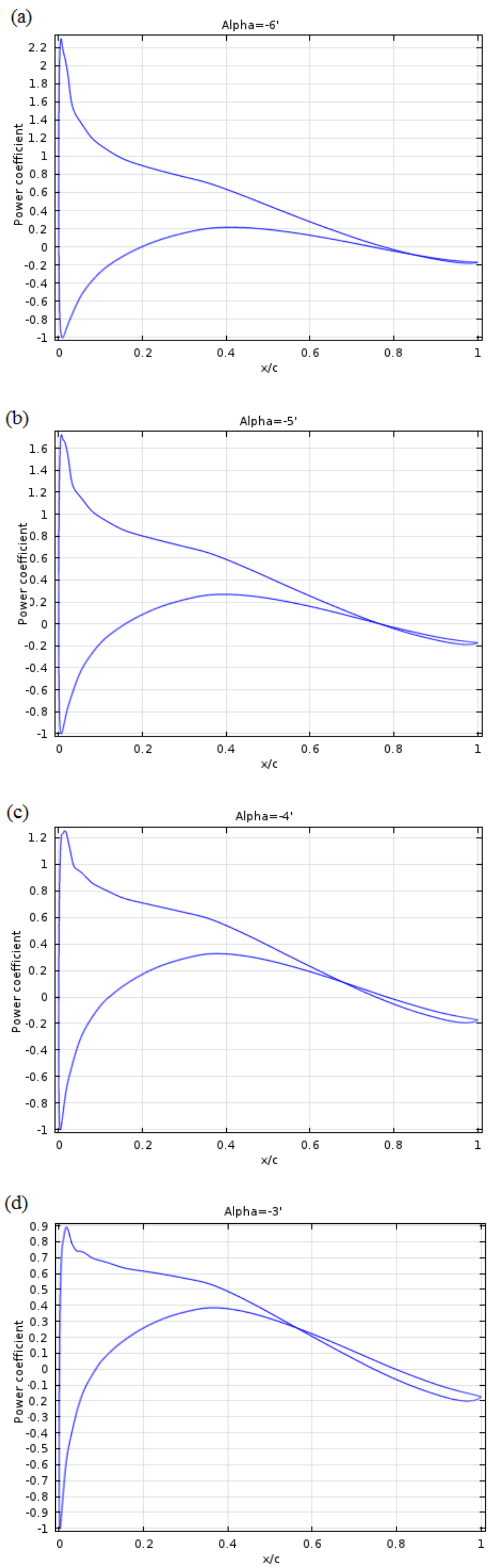

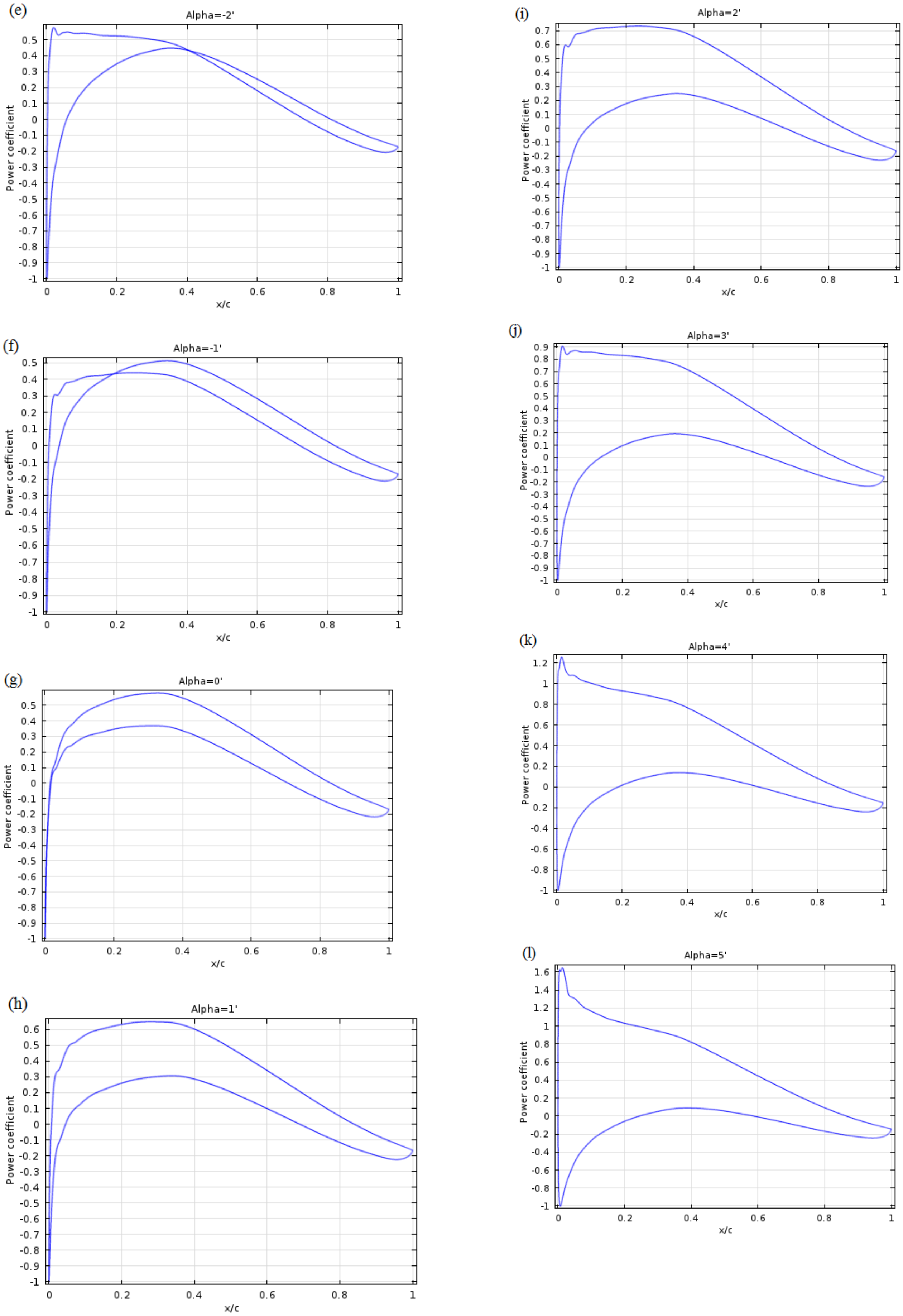
(e)
Alpha=-2'
Power coefficient
x/c
(f)
Alpha=-1'
Power coefficient
x/c
(g)
Alpha=0'
Power coefficient
x/c
(h)
Alpha=1'
Power coefficient
x/c
(i)
Alpha=2'
Power coefficient
x/c
(j)
Alpha=3'
Power coefficient
x/c
(k)
Alpha=4'
Power coefficient
x/c
(l)
Alpha=5'
Power coefficient
x/c

(m)
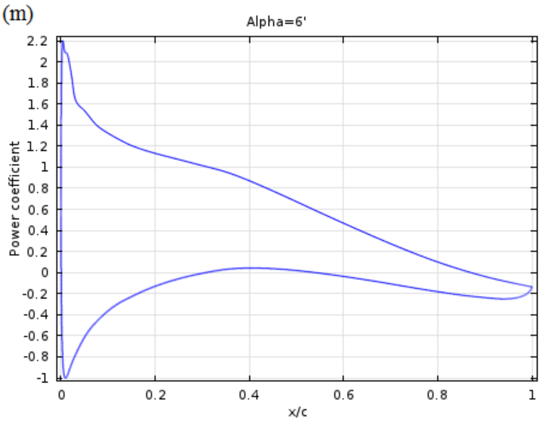

(n)
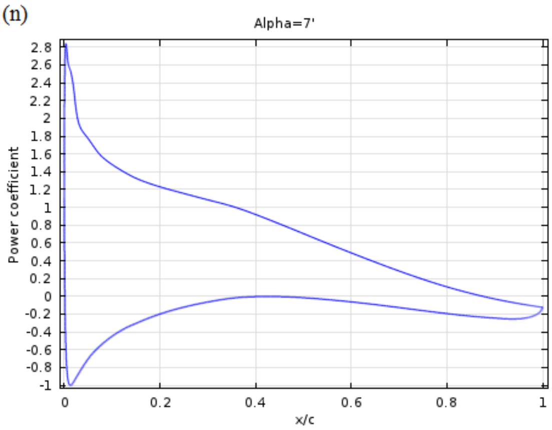

(o)
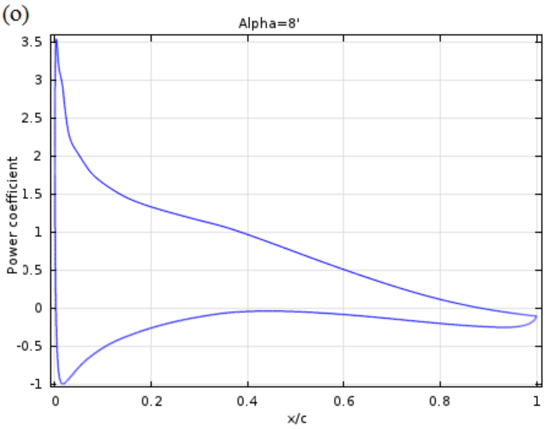

(p)
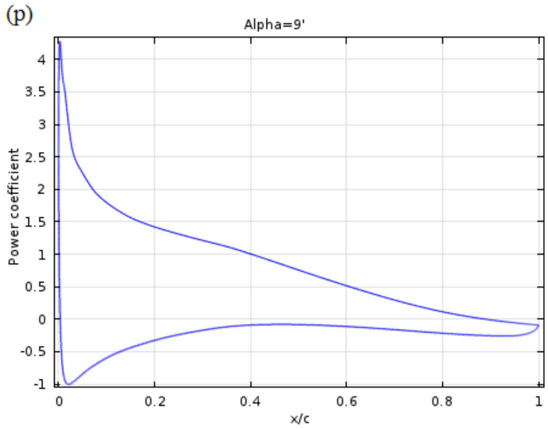

(r)
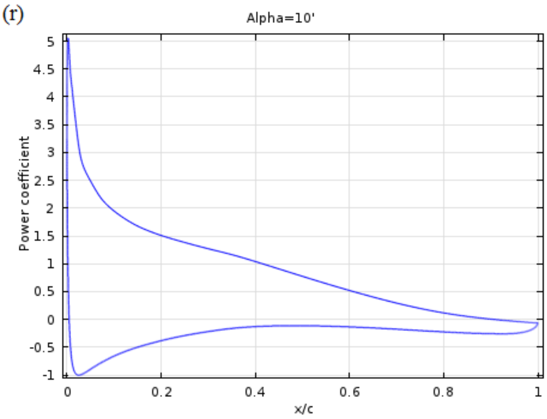

Figure 6a-r. Pressure coefficient of NACA NACA 632-215 airfoils with different angle of attack.

As can be seen from the Figure 6a-r, with the decreasing angle of attack from -6 to 0 degree, pressure difference between upper and lower surface decreases. After zero degree with the increasing of angle, pressure difference between upper and lower surface starts to increase again. Around -1 to 0 degree pressure difference between upper and lower surface reach minimum and at 10 degree becomes maximum.

IV. CONCLUSION

This paper numerically investigates optimum angle of attack for NACA 63_2-215 airfoil to find maximum lift to drag ratio for five wind speed cases. This study simulates air flow around inclined NACA 63_2-215 airfoil using SST turbulence model. Initially airfoil simulated at the speed from 10 to 50 m/s and results were compared. Lift, drag coefficient, lift to drag ratio and power coefficient around the airfoil were calculated and compared with different velocity. With the increasing of wind velocity, lift and drag coefficient increases. Maximum lift to drag ratio starts to increase then degreases again. Maximum lift to drag ratio is reached around 4 degree. Power coefficients were calculated at the speed of 10 m/s and graph was plotted. With the increasing angle of attack, pressure difference between upper and lower surface increases. As a result, with the increasing of speed of air, lift and drag coefficient increases with respect to angle, maximum lift to drag ratio is reached around 4 degree and lift coefficients are minus at the angle of -4 to -7.

ACKNOWLEDGMENT

I thank Middle East Technical University, allowing me to to this work in there with their facility.

NOMENCLATURE

C_P Pressure coefficient
C_L Lift coefficient
P Static pressure
P_∞ Free stream pressure
U_r Relative velocity
U_∞ Free stream velocity (wind velocity)
u Velocity fiel x component
v Velocity fiel y component
c Airfoil chord

t Percentage of the maximum thickness
k Turbulence kinetic energy
l_{ref} Reference length scale
ε Turbulence dissipation rate
ω Rotational velocity
ρ Density
ρ_∞ Freestream density
μ Dynamic viscosity
μ_{eff} Effective dynamic viscosity
α Angle of attack

REFERENCES

[1] EWEA, European Wind Energy Association, Wind in power: 2014 European statistics http://www.ewea.org/

[2] S. Rajakumar, D. Ravindran, "Computational fluid dynamics of windturbine blade at various angles of attack and low reynolds number", International Journal of Engineering Science and Technology Vol. 2 ,11, 2010, pp. 6474-6484.

[3] K.S. Lee, C.H. Chung b, J.H. Baek, "Lift correction model for local shear flow effect on wind turbine airfoils", Renewable Energy 65, 2014, pp. 275-280.

[4] K. Gharali, D.A. Johnson, "Numerical modeling of an S809 airfoil under dynamic stall, erosion and high reduced frequencies", Applied Energy 93, 2012, pp. 45–52.

[5] C. Thumthae, T. Chitsomboon, "Optimal angle of attack for untwisted blade wind turbine", Renewable Energy 34, 2009, pp. 1279–1284.

[6] S.G. Lee, S.J. Park, K.S. Lee, "Chinwha Chung, Performance prediction of NREL (National Renewable Energy Laboratory) Phase VI blade adopting blunt trailing edge airfoil", Energy 47, 2012, pp. 47-61.

[7] A. Zanottin, R. Nilifard, G. Gibertini, A. Guardone, G. Quaranta, "Assessment of 2D/3D numerical modeling for deep dynamic stall experiments", Journal of Fluids and Structures 51, 2014, pp. 97–115.

[8] COMSOL CFD module user guide. http://www.comsol.com. 2015.